THE EFFECTS OF LOSSY FREQUENCY-DOMAIN EEG COMPRESSION ON CROSS-FREQUENCY COUPLING ANALYSIS

Andrew J. Phillips
Klipsch School of Electrical and Computer Engineering
New Mexico State University
Las Cruces, NM, USA
andrew88@nmsu.edu

Faculty Advisor:
Dr. Charles D. Creusere
ccreuser@nmsu.edu

ABSTRACT

This paper analyzes lossy frequency-domain compression in the context of cross-frequency coupling (CFC) analysis of electroencephalograph (EEG) signals. The approach used here for CFC analysis involves a low-complexity signal analysis block followed by a constant false alarm rate (CFAR) detection algorithm. The lossy frequency-domain compression is achieved via the threshold coding method for frequency truncation using the discrete cosine transform (DCT). This method is found to increase CFC detection rates by as much as 30% to 50% depending on the amount of Gaussian noise in the signal and the selected probability of false alarm. Further analysis indicates that these significant improvements in CFC detection rates are due to adaptive frequency-domain noise reduction. These results bode well for lossy frequency-based EEG compression schemes which can greatly improve transmission speeds and decrease storage space requirements while simultaneously enhancing CFC analysis capabilities.

INTRODUCTION

A major new vision within the neuroscience community is the concept of cross-frequency coupling (CFC) in electroencephalograph (EEG) data. CFC is the result of complex interactions of neural populations, each of which manifests certain oscillatory behaviors in select frequency ranges. Structural cross-frequency relationships have been found to hold a functional role in the execution of cognitive functions such as decision making, communication, and learning [1, 2, 3]. Although cross-frequency relationships come in a variety of forms, the most extensively studied relationship in the literature is phase-amplitude coupling (PAC), whereby the amplitude of high-frequency oscillations is modulated by the phase of low-frequency rhythms. PAC research commonly focuses on the interaction of the phase of low-frequency theta rhythms (5-10 Hz) with the

amplitude of gamma (30-80 Hz) and high gamma (80-200 Hz) oscillations [4, 5, 6], with theoretical work suggesting that theta-gamma PAC is involved in sequential memory organization and the maintenance of working memory [7]. Thus, the amount of CFC between theta phase and gamma amplitude as well as the exact combination of theta and gamma subbands gives us insight regarding information processing and storage activities within the brain. Recent research is using changes in PAC as an indication of neurological disorders including schizophrenia, obsessive-compulsive disorder, Alzheimer's disease, epilepsy, and Parkinson's disease, and is even considering the potential of CFC as a therapeutic target in disease states [8].

The increasing prevalence of processing EEG datasets for diagnostic purposes has provoked further consideration regarding the compression of EEG data to improve transmission speeds and decrease storage space requirements. Many EEG compression methodologies studied to date have been lossless or near-lossless [9, 10, 11] due to clinical liability considerations. However, the entropy of the EEG signal limits the maximum compression achievable for lossless schemes. Lossy compression schemes can overcome this issue as long as we ensure that diagnostically significant data remains intact. A recent investigation of the effects of lossy compression on event-related potential (ERP) analysis of EEG data demonstrated that lossy compression is a feasible option for EEG datasets destined for ERP analysis [12]. In a similar manner, this paper investigates the degree to which lossy compression affects CFC analysis of EEG signals.

METHODS

A. Generating Cross-Frequency Coupled EEG Signals

The EEG signals used for this research were synthesized using the program developed by Tort et al. [6]. The plots in this paper reference a 10-second synthesized EEG signal with a 1024 Hz sampling rate containing CFC between a low-frequency theta rhythm centered at 10 Hz and a high-frequency high gamma oscillation centered at 108 Hz, with the purpose of obtaining results applicable to the theta-gamma coupling domain [4, 5]. Note that results similar to those presented here were obtained for other cross-frequency coupled signals as well. For some experiments, Gaussian noise was added to the synthesized EEG signal to simulate the noise present in real-world EEG signals. View the left hand side of Figure 8 for 1 second segments of synthesized EEG signals containing additive Gaussian noise with standard deviation of 0, 1, and 2.

B. CFC Analysis

A number of approaches have been proposed to quantify the amount of CFC present in an EEG signal [13, 14, 15, 16, 17], yet no single method has been chosen as the gold standard [3]. Creusere, McRae, & Davis [18] recently introduced a new approach for CFC analysis that is used in this research. In particular, this method detects phase-amplitude coupling and the reader may assume from this point forward that any mention of CFC is of the PAC variety. The approach consists of a low-complexity signal analysis block (Figure 1) that is well-suited for implementation as an integrated circuit followed by constant false alarm rate (CFAR) detection (Figure 2). The output CFC signals from Figure 1 are used for CFAR detection in Figure 2.

The low and high band filters of Figure 1 are narrow bandpass filters implemented as short

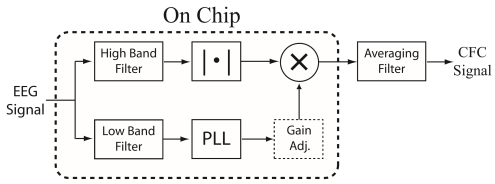

Figure 1: Sample-based CFC analysis block as proposed by [18].

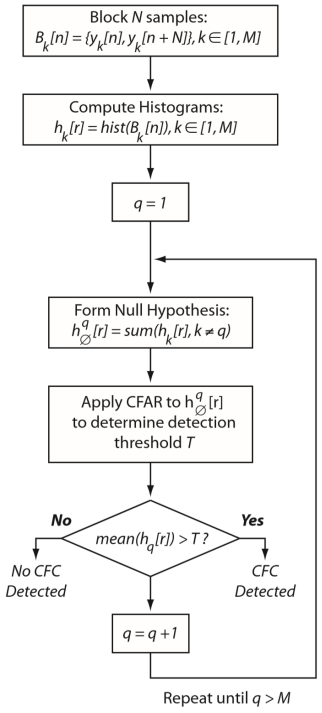

Figure 2: CFAR detection approach as proposed by [18]. Blocks of N samples are collected from each of the M CFC channels and histograms are computed. For each channel, a null hypothesis histogram is formed, a CFAR threshold is calculated, and a detection decision is made.

cascades of simple 2nd order IIR filters using Direct Form 2 structures. In total, Creusere et al. defined 15 high band filters in the gamma and high-gamma ranges specified in intervals of 10 Hz beginning at 38 Hz and ending at 178 Hz. CFC detection decisions are made for a low-frequency rhythm query (e.g. 10 Hz) on 200-sample blocks of the CFC signal for each high band filter. For the results below, the CFC detection rate for a given synthesized EEG signal was calculated by passing the 10 Hz low-frequency rhythm query to the CFAR detection algorithm and determining the number of blocks that detected CFC out of the total number of blocks in the CFC signal for the 108 Hz high band filter.

C. EEG Data Compression

The method of lossy data compression investigated here is frequency truncation using the discrete cosine transform (DCT), a popular choice to perform signal compression due to its strong

energy compaction property. To compress an arbitrary 10-second synthesized EEG signal, we computed the DCT-IV for each 1-second block in the synthesized EEG signal by

$$y(k) = \sqrt{\frac{2}{N}} \sum_{n=1}^{N} x(n) cos(\frac{\pi}{4N}(2n-1)(2k-1)) \tag{1}$$

where $x(n)$ is the 1-second block in the synthesized EEG signal and $N = 1024$. For each block transform, we used the method of threshold coding to retain a percentage of the DCT-IV coefficients with the greatest energy and zeroed out the remainder. We then computed the inverse of the DCT-IV for each block transform by

$$x(n) = \sqrt{\frac{2}{N}} \sum_{k=1}^{N} y(k) cos(\frac{\pi}{4N}(2k-1)(2n-1)) \tag{2}$$

resulting in a compressed version of the synthesized EEG signal after concatenating the compressed 1-second blocks in the appropriate order.

The general approach taken to determine CFC detection rates for varying degrees of lossy compression is depicted in Figure 3. Following selection of the probability of false alarm (PFA) for CFAR detection and the amount of Gaussian noise to add to the synthesized EEG signal, a Monte Carlo simulation was performed using M independently synthesized EEG signals. Each independently synthesized EEG signal was compressed to varying degrees, and each of the resulting signals underwent CFC detection as described in Subsection B. above. For the experiments shown below, we iterated over PFAs of 0.001, 0.01, 0.1, and 0.2 and additive Gaussian noise with standard deviations of 0, 1, and 2. Each Monte Carlo simulation consisted of 100 iterations unless otherwise noted.

RESULTS

D. Effects of Additive Gaussian Noise on CFC Detection Rates

Figure 4 displays the effect of the additive Gaussian noise on the CFAR detection rate at PFAs of 0.001, 0.01, 0.1, and 0.2. The trends in Figure 4 confirm that the CFC algorithm and CFAR detection work as expected. First, we anticipate that increasing the PFA should also increase the CFC detection rate, since the detection threshold on the null hypothesis distribution would become less stringent. In fact, this is exactly what we observe in Figure 4 as increasing the PFA monotonically increases the CFC detection rate across all levels of additive Gaussian noise. Second, we anticipate that increasing the standard deviation of the additive Gaussian noise should decrease the CFC detection rate, since more noise power in the signal leads to a smaller signal-to-noise ratio. Again, we observe this trend in Figure 4 as increasing the standard deviation of the additive Gaussian noise leads to monotonically decreasing CFC detection rates.

E. Effects of Frequency Truncation on CFC Detection Rates

Figure 5 displays the CFC detection rate as a function of the percentage of DCT coefficients discarded using the threshold coding method for frequency truncation. The CFC detection rates

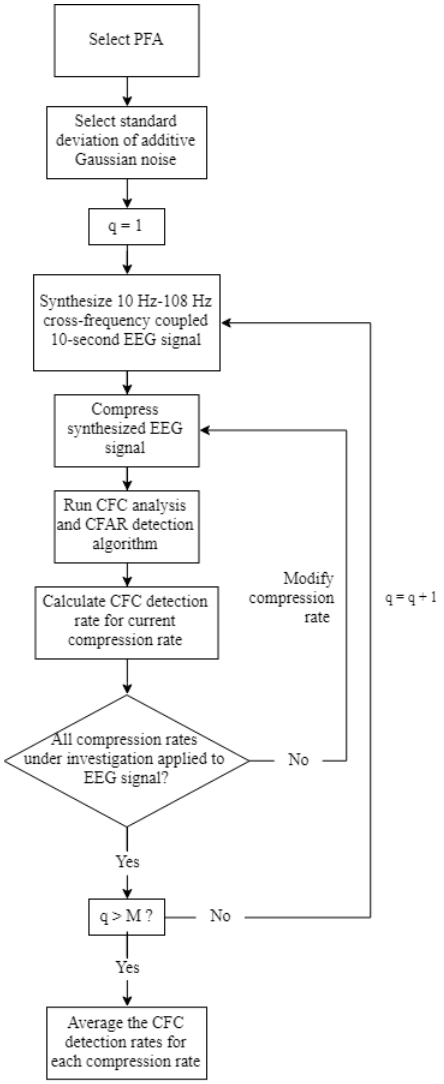

Figure 3: Monte Carlo simulation process consisting of M iterations that determined CFC detection rates at various configurations of the PFA and additive Gaussian noise.

are computed for between 0% and 100% of DCT coefficients discarded in increments of 10%. The families of plots sharing the same color represent common PFAs and the families of plots sharing the same line style represent common levels of additive Gaussian noise. In accordance with our observations in Figure 4, we see that increasing the standard deviation of additive Gaussian noise leads to lower CFC detection rates. Likewise, we can confirm that increasing the PFA leads to higher CFC detection rates. Note that the plot for *PFA .2, Noise Std Dev 0* obscures the other plots with *Noise Std Dev 0*, that is, all plots with no additive Gaussian noise (regardless of the PFA) detect CFC at the maximum possible rate until 100% of the DCT coefficients are discarded.

It was expected that an increase in the amount of frequency truncation would lead to a decrease in CFC detection rates due to information loss. On the contrary, the trends demonstrate the opposite of this prediction. That is, we observe that as the amount of frequency truncation increases, there is a corresponding monotonic *increase* in the CFC detection rate until 100% of the DCT coefficients

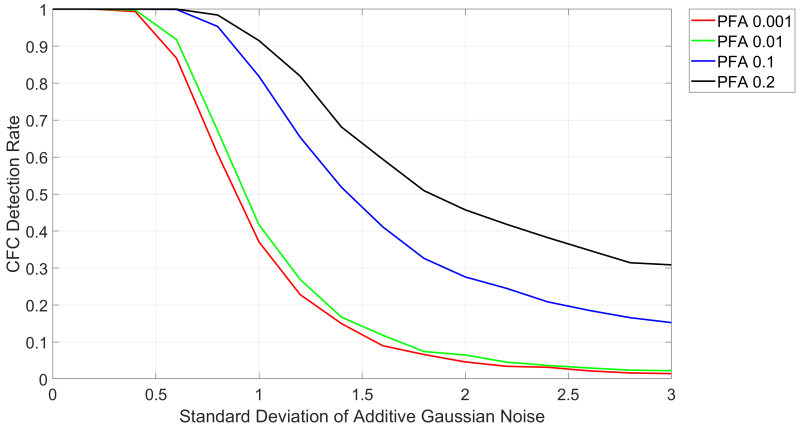

Figure 4: CFC detection rate as a function of additive Gaussian noise.

are discarded, at which point the CFC detection rate bottoms out at 0% (as it must, regardless of the particular combination of PFA and additive Gaussian noise).

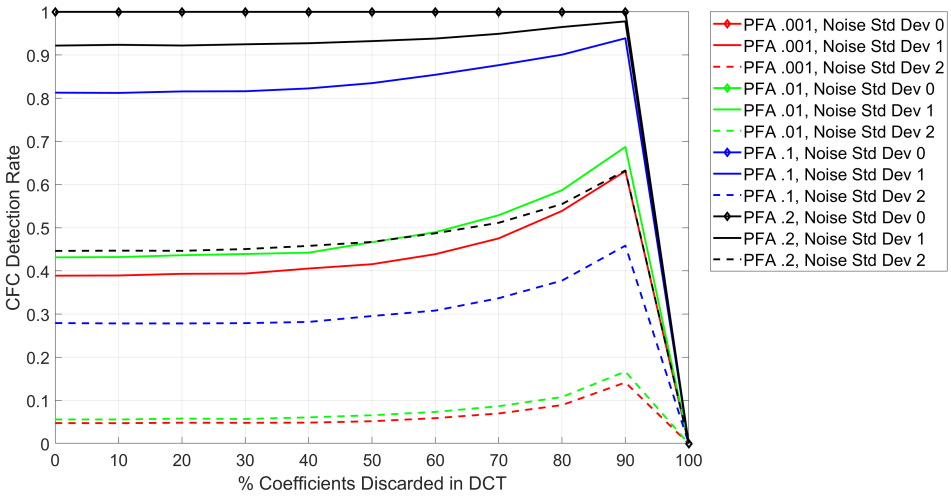

Figure 5: CFC detection rate as a function of frequency truncation.

F. Maximum CFC Detection Rates For Frequency Truncation

To inspect the maxima of these plots with greater precision, we increased the fidelity of the results at high rates of frequency truncation. Figure 6 displays CFC detection rates for between 99.1% and 100% of DCT coefficients discarded in increments of 0.1% . Considering Figures 5 and 6 together, we see that frequency truncation using the DCT increases CFC detection rates for noisy EEG signals by as much as 30% to 50% depending on the particular combination of PFA and additive Gaussian noise. For example, the plot for *PFA .001, Noise Std Dev 1* has a CFC detection rate of approximately 0.4 or 40% for 0% of DCT coefficients discarded and a CFC detection rate

of approximately 0.9 or 90% for 99.5% of DCT coefficients discarded, demonstrating an increase in the CFC detection rate of around 0.5 or 50%.

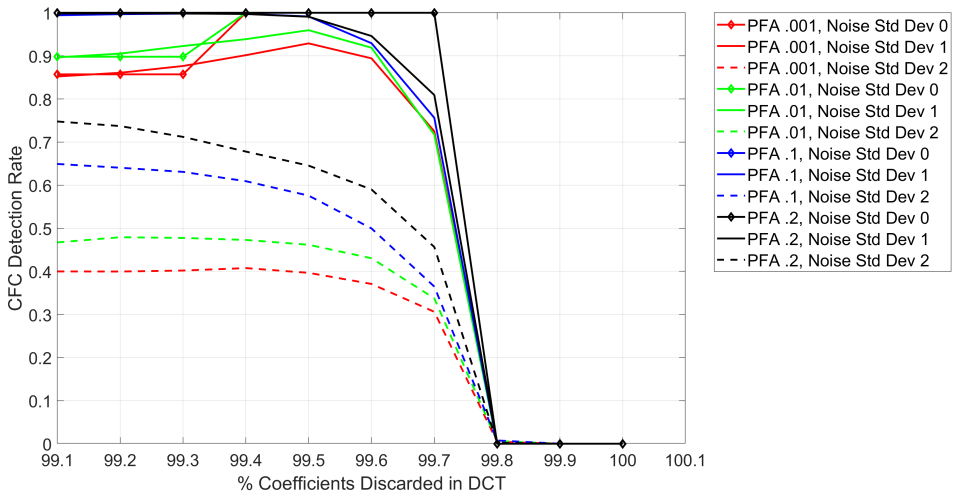

Figure 6: CFC detection rate as a function of frequency truncation from 99.1% to 100% of DCT coefficients discarded.

While not all plots achieve a maximum at exactly the same truncation rate, we selected an appropriately representative truncation rate of 99.5% of coefficients discarded in the DCT for further investigation. A Monte Carlo simulation of 10000 iterations was used to determine the indices of the retained DCT coefficients at the truncation rate of 99.5% for each of the various levels of additive Gaussian noise. The results are displayed in Figure 7. Note that only those DCT coefficients that were retained more than 1% of the time are considered in these graphs. It is clear that the commonly retained DCT coefficients around indices 20 and 21 correspond to the low-frequency theta rhythm centered at 10 Hz, and that the commonly retained DCT coefficients around index 216 correspond to the high-frequency high gamma oscillation centered at 108 Hz. The cases with no additive Gaussian noise always retain the same DCT coefficients, while increasing the Gaussian noise diversifies the distributions. However, observe that the distributions remain clustered around the indices described above regardless of the amount of additive Gaussian noise in the synthesized cross-frequency coupled EEG signals.

DISCUSSION

The data in Figure 7 suggest that the significant improvements in CFC detection rates at high compression rates may be due to adaptive frequency-domain noise reduction. To gain further insight, Figure 8 displays the synthesized EEG signals in the time-domain with different levels of additive Gaussian noise before and after frequency truncation at the truncation rate of 99.5% of DCT coefficients. Note that the frequency-truncated cross-frequency coupled EEG signals approach a standard form, regardless of the additive Gaussian noise in the synthesized EEG signals. This noise reduction allows one to visually detect the cross-frequency coupled nature of the synthesized EEG signals much more easily. Further, and more importantly, this noise reduction also

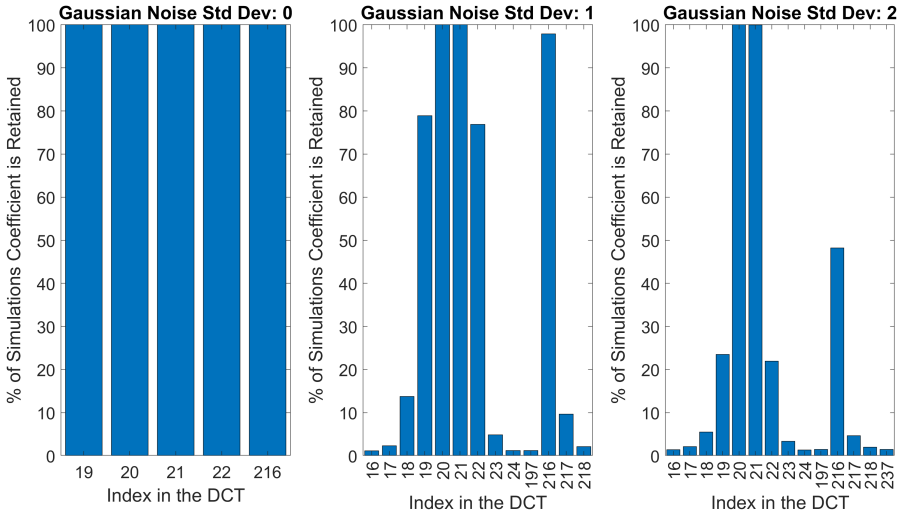

Figure 7: Indices of the DCT coefficients retained at truncation rate 99.5% for various levels of additive Gaussian noise as determined by Monte Carlo simulations. Note the distribution around indices 20 and 21 corresponding to the 10 Hz low-frequency theta rhythm and the distribution around index 216 corresponding to the 108 Hz high-frequency high gamma oscillation.

aids the CFC analysis and CFAR detection algorithms developed by [18] in properly identifying instances of CFC.

The intersection of this adaptive frequency-domain noise reduction with cross-frequency coupling analysis has been sparsely explored, although the results appear promising. At least one other study [19] has demonstrated improvements in CFC metrics via variable bandwidth filters for noise reduction, although performance was not evaluated using CFAR detection.

CONCLUSIONS

In this paper, we have considered the effect that lossy frequency-domain compression has on CFC analysis of EEG signals. In particular, we investigated the impact that the threshold coding method for frequency truncation using the DCT has on the CFC analysis and CFAR detection algorithms put forth by Creusere et al. [18]. We found that frequency truncation using the DCT increases CFC detection rates for noisy EEG signals by as much as 30% to 50% depending on the PFA and the additive Gaussian noise. Thus, lossy frequency-domain compression appears not only tolerable for real-world EEG signals destined for CFC detection, but even favorable due to the observed improvement in CFC detection capabilities. These results motivate utilization of the compression scheme presented above for EEG datasets focused on CFC detection. Future work includes investigating the effects of other lossy compression schemes on cross-frequency coupling analysis of EEG signals.

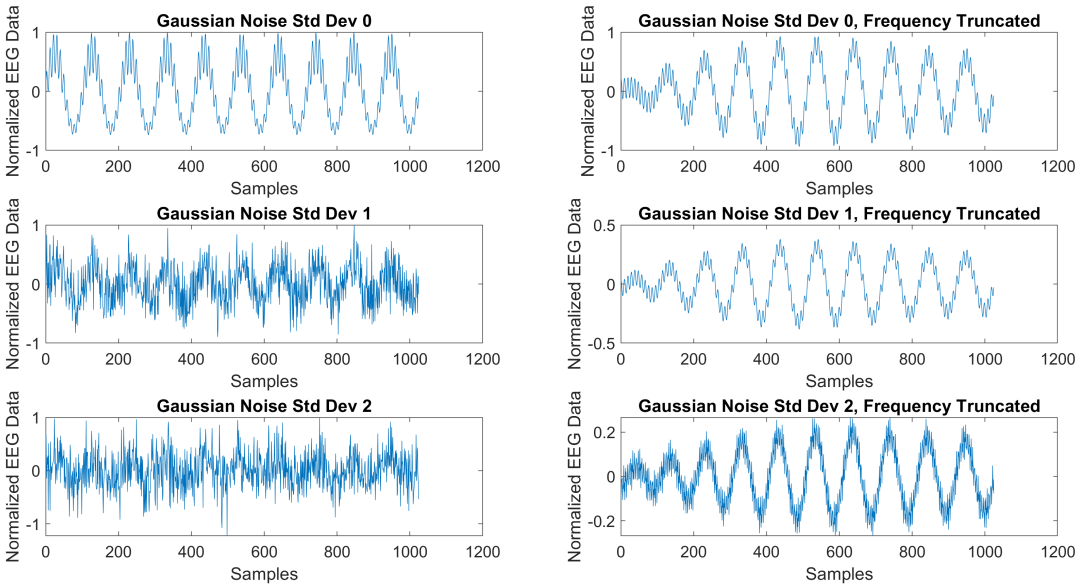

Figure 8: Synthesized cross-frequency coupled EEG signals in the time-domain with different levels of additive Gaussian noise (left) before and after frequency truncation at the truncation rate of 99.5% of DCT coefficients (right). Note how the frequency-truncated cross-frequency coupled EEG signals approach a standard form as a result of the adaptive frequency-domain noise reduction.

REFERENCES

[1] F. Varela, J.-P. Lachaux, E. Rodriguez, and J. Martinerie, "The brainweb: Phase synchronization and large-scale integration," *Nature Reviews Neuroscience*, vol. 2, no. 4, p. 229239, 2001.

[2] A. K. Engel, P. Fries, and W. Singer, "Dynamic predictions: Oscillations and synchrony in topdown processing," *Nature Reviews Neuroscience*, vol. 2, no. 10, p. 704716, 2001.

[3] R. T. Canolty and R. T. Knight, "The functional role of cross-frequency coupling," *Trends in Cognitive Sciences*, vol. 14, no. 11, pp. 506 – 515, 2010.

[4] R. T. Canolty, E. Edwards, S. S. Dalal, M. Soltani, S. S. Nagarajan, H. E. Kirsch, M. S. Berger, N. M. Barbaro, and R. T. Knight, "High gamma power is phase-locked to theta oscillations in human neocortex," *Science*, vol. 313, no. 5793, pp. 1626–1628, 2006.

[5] O. Jensen and L. L. Colgin, "Cross-frequency coupling between neuronal oscillations," *Trends in Cognitive Sciences*, vol. 11, no. 7, pp. 267 – 269, 2007.

[6] A. B. L. Tort, R. Komorowski, H. Eichenbaum, and N. Kopell, "Measuring phase-amplitude coupling between neuronal oscillations of different frequencies," *Journal of Neurophysiology*, vol. 104, no. 2, pp. 1195–1210, 2010. PMID: 20463205.

[7] J. Lisman, "The theta/gamma discrete phase code occuring during the hippocampal phase precession may be a more general brain coding scheme," *Hippocampus*, vol. 15, no. 7, pp. 913–922, 2005.

[8] Y. Salimpour and W. S. Anderson, "Cross-frequency coupling based neuromodulation for treating neurological disorders," *Frontiers in Neuroscience*, vol. 13, 2019.

[9] N. Memon, X. Kong, and J. Cinkler, "Context-based lossless and near-lossless compression of EEG signals," *IEEE Transactions on Information Technology in Biomedicine*, vol. 3, pp. 231–238, September 1999.

[10] G. Antoniol and P. Tonella, "EEG data compression techniques," *IEEE Transactions on Biomedical Engineering*, vol. 44, pp. 105–114, February 1997.

[11] G. D. y. Álvarez, F. Favaro, F. Lecumberry, Á. Martín, J. P. Oliver, J. Oreggioni, I. Ramírez, G. Seroussi, and L. Steinfeld, "Wireless EEG system achieving high throughput and reduced energy consumption through lossless and near-lossless compression," *IEEE Transactions on Biomedical Circuits and Systems*, vol. 12, pp. 231–241, Feb 2018.

[12] A. J. Phillips and C. D. Creusere, "The effects of lossy eeg compression on erp analysis," *International Telemetering Conference Proceedings*, 2018.

[13] A. Bruns and R. Eckhorn, "Task-related coupling from high- to low-frequency signals among visual cortical areas in human subdural recordings," *International Journal of Psychophysiology*, vol. 51, no. 2, pp. 97 – 116, 2004.

[14] P. Lakatos, A. S. Shah, K. H. Knuth, I. Ulbert, G. Karmos, and C. E. Schroeder, "An oscillatory hierarchy controlling neuronal excitability and stimulus processing in the auditory cortex," *Journal of Neurophysiology*, vol. 94, no. 3, pp. 1904–1911, 2005. PMID: 15901760.

[15] W. Penny, E. Duzel, K. Miller, and J. Ojemann, "Testing for nested oscillation," *Journal of Neuroscience Methods*, vol. 174, no. 1, p. 5061, 2008.

[16] A. B. L. Tort, M. A. Kramer, C. Thorn, D. J. Gibson, Y. Kubota, A. M. Graybiel, and N. J. Kopell, "Dynamic cross-frequency couplings of local field potential oscillations in rat striatum and hippocampus during performance of a t-maze task," *Proceedings of the National Academy of Sciences*, vol. 105, no. 51, pp. 20517–20522, 2008.

[17] M. X. Cohen, "Assessing transient cross-frequency coupling in eeg data," *Journal of Neuroscience Methods*, vol. 168, no. 2, p. 494499, 2008.

[18] C. D. Creusere, N. McRae, and P. Davis, "Sample-based cross-frequency coupling analysis with cfar detection," *2014 48th Asilomar Conference on Signals, Systems and Computers*, pp. 179–183, Nov 2014.

[19] J. I. Berman, J. Mcdaniel, S. Liu, L. Cornew, W. Gaetz, T. P. Roberts, and J. C. Edgar, "Variable bandwidth filtering for improved sensitivity of cross-frequency coupling metrics," *Brain Connectivity*, vol. 2, no. 3, p. 155163, 2012.